Continuous-Flow Catalysis Using Phosphine-Metal Complexes on Porous Polymers: Designing Ligands, Pores, and Reactors

Matsumoto, Hikaru
Department of Chemical Engineering, Faculty of Engineering, Kyushu University

Iwai, Tomohiro
Department of Basic Science, Graduate School of Arts and Sciences, The University of Tokyo

Sawamura, Masaya
Institute for Chemical Reaction Design and Discovery (WPI-ICReDD), Hokkaido University

Miura, Yoshiko
Department of Chemical Engineering, Faculty of Engineering, Kyushu University

https://hdl.handle.net/2324/7178743

KYUSHU UNIVERSITY

ChemPlusChem

Review
doi.org/10.1002/cplu.202400039
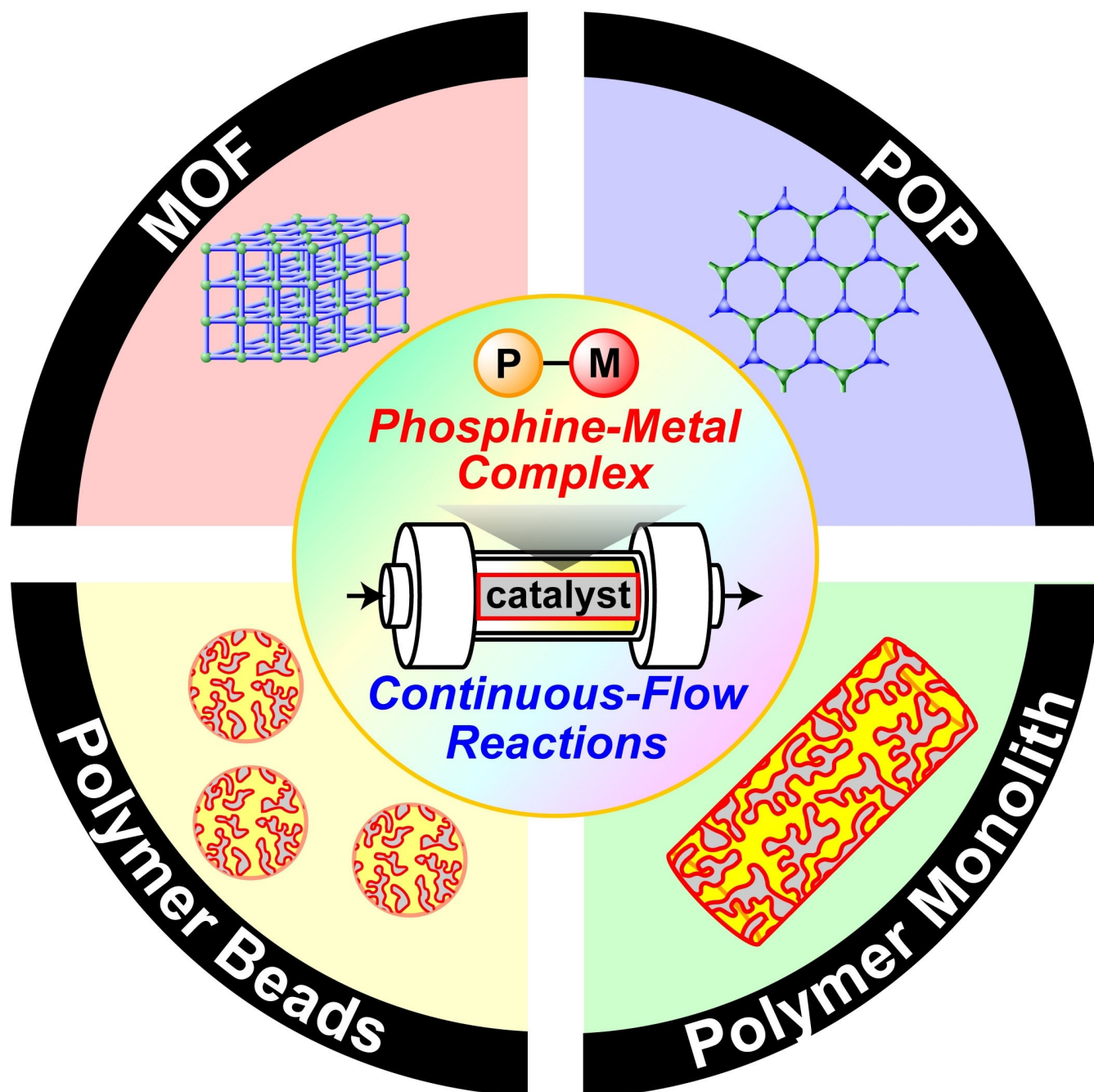
Chemistry Europe
European Chemical Societies Publishing

www.chempluschem.org

Continuous-Flow Catalysis Using Phosphine-Metal Complexes on Porous Polymers: Designing Ligands, Pores, and Reactors

Hikaru Matsumoto,[a] Tomohiro Iwai,[b] Masaya Sawamura,*[c, d] and Yoshiko Miura*[a]

Continuous-flow syntheses using immobilized catalysts can offer efficient chemical processes with easy separation and purification. Porous polymers have gained significant interests for their applications to catalytic systems in the field of organic chemistry. The porous polymers are recognized for their large surface area, high chemical stability, facile modulation of surface chemistry, and cost-effectiveness. It is crucial to immobilize transition-metal catalysts due to their difficult separation and high toxicity. Supported phosphine ligands represent a noteworthy system for the effective immobilization of metal catalysts and modulation of catalytic properties.

Researchers have been actively pursuing strategies involving phosphine-metal complexes supported on porous polymers, aiming for high activities, durabilities, selectivities, and applicability to continuous-flow systems. This review provides a concise overview of phosphine-metal complexes supported on porous polymers for continuous-flow catalytic reactions. Polymer catalysts are categorized based on pore sizes, including micro-, meso-, and macroporous polymers. The characteristics of these porous polymers are explored concerning their efficiency in immobilized catalysis and continuous-flow systems.

1. Introduction

Continuous-flow reactions are attracting significant attention as novel synthetic tools in the field of organic chemistry due to numerous advantages over batch systems.[1] The benefits of the continuous-flow system are truly evident when considering reaction conditions and reactor geometries. For example, micro- or milliflow reactors often provide efficient heat exchange, good mixing, and precise control over reaction time. These advantages have been theoretically studied based on fluid dynamics.[1c] Moreover, continuous-flow systems facilitate early-stage scale-out of reactions, allowing for effective on-demand production in compact and reconfigurable setups. These setups can be seamlessly integrated with computer- and/or artificial intelligence (AI)-aided automated systems.[2] Particularly, continuous-flow synthesis using immobilized catalyst, where the catalytic species is supported on a solid material and securely fixed in a reactor, is desired to enable catalytic reactions while simultaneously facilitating efficient separations between catalysts and reaction solution.[3]

One drawback of immobilized catalysts is relatively lower catalytic activities and selectivities compared with those of their homogeneous counterparts. To address these challenges, porous materials have emerged as promising solutions, show-casing success in immobilized catalysis due to their intriguing structures featuring large surface areas, size-selective incorporation of guest molecules, and permanent porosity for improved mass transport and selective molecular conversions.[4] IUPAC recommendations classify pores into micro- (<2 nm), meso- (2–50 nm), and macropores (>50 nm).[5] The microporous structures of support materials play a crucial role in enhancing catalytic durability and selectivity. Single-site catalytic centers and size-controlled pore networks become pivotal and can be designed based on the chemical structures of precursors.[4] On the other hand, meso- and macropores primarily influence mass transfer and fluid dynamics on immobilized catalysts. In continuous-flow applications, the hydrodynamic properties within a column reactor are key factors for efficient mass transport on immobilized catalysts.[6] Several types of porous materials have indeed demonstrated their feasibility in organic reactions in continuous-flow systems.

The concept of the immobilized catalysts is pivotal in organic syntheses using transition metals, addressing challenges such as high costs, difficult separation, and high toxicity. Effectively heterogenizing and modulating metal catalysts can be achieved by introducing supported ligands on insoluble materials. Researchers often prioritize inorganic materials for immobilized transition-metal catalysts due to their superior thermal and physical stability. Among these, silica-based catalysts stand out as representative due to their wide accessibility, various processing methods, excellent thermal stability, tunable porosity and size, and the availability of surface modification for introducing ligands.[7] On the other hand, synthetic polymers have played a crucial role in advancing immobilized catalysts, offering high chemical stability, easy chemical functionalization, and cost-effectiveness.[8] Synthetic polymers allow the incorporation of functional groups through surface-grafting, co-polymerization, or encapsulation methods. Various types of polymer-supported ligands have been developed using linear polymers,[9] polymer resins,[10] polymer capsules,[11] and porous polymers[4] for diverse transition-metal catalysis.

Tertiary phosphines stand out as the most widely utilized organic ligands for various catalytically important transition metals, including Ru, Ir, Rh, Pd, Ni, and Co, as seen in the wide range of immobilized catalysis such as hydrogenations,[12] hydroformylations,[13] oxidations,[14] cross-couplings,[15] metatheses,[16] and so on. By carefully tuning the chemical

[a] Dr. H. Matsumoto, Prof. Dr. Y. Miura
Department of Chemical Engineering, Faculty of Engineering
Kyushu University
744 Motooka, Nishi-ku, Fukuoka 819-0395 (Japan)
E-mail: miuray@chem-eng.kyushu-u.ac.jp

[b] Dr. T. Iwai
Department of Basic Science, Graduate School of Arts and Sciences
The University of Tokyo
3-8-1 Komaba, Meguro-ku, Tokyo 153-8902 (Japan)

[c] Prof. Dr. M. Sawamura
Institute for Chemical Reaction Design and Discovery (WPI-ICReDD)
Hokkaido University
Kita 21, Nishi 10, Kita-ku, Sapporo 001-0021 (Japan)

[d] Prof. Dr. M. Sawamura
Department of Chemistry, Faculty of Science
Hokkaido University
Kita 10 Nishi 8, Kita-ku, Sapporo 060-0810 (Japan)
E-mail: sawamura@sci.hokudai.ac.jp

ChemPlusChem

Review
doi.org/10.1002/cplu.202400039

Chemistry Europe
European Chemical
Societies Publishing

structure of substituents on the phosphorus atom, the steric and electronic properties around the ligated metal center can be modulated to tailor the reactivity and selectivity of the catalytic system. The exploration of catalytic systems featuring a variety of phosphine-metal complexes has progressed significantly, especially when combined with porous materials. Comprehensive reviews on phosphine-metal complexes supported on porous polymers have thoughtfully published elsewhere.[4,17]

Porous polymers can be systematically categorized based on their pore sizes. The micropores of metal organic frameworks (MOFs), covalent organic frameworks (COFs), and porous organic polymers (POPs) prove advantageous hosting single-site catalytic centers and size-controlled pores, thereby enhancing catalytic performance. These polymers are meticulously designed based on the chemical structures of precursors (Figure 1a). In terms of the hydrodynamic and mass transfer properties crucial for continuous-flow reactors, macroporous polymer beads and monoliths have demonstrated significant potential (Figure 1b). This review focuses specifically on the continuous-flow applications of porous polymer catalysts. The design of porous structures featuring supported phosphine ligands, continuous-flow reactor systems, and catalytic performances of the immobilized catalysts will be briefly summarized.

2. Micro- and Mesoporous Polymers

In the past decades, the field of porous materials has experienced revolutionary growth, witnessing the emergence of novel materials such as MOFs,[18] COFs,[19] and POPs.[20] These porous materials exhibit unique properties, extensively docu-
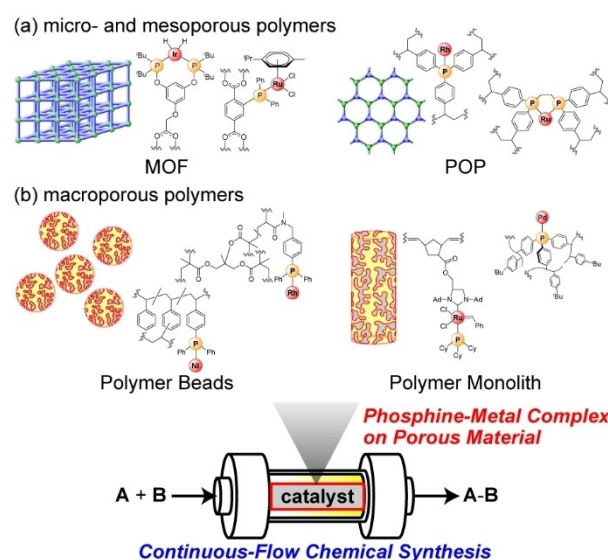

Figure 1. Porous polymers containing phosphine-metal complexes as immobilized catalysts for continuous-flow reactions.

mented for their tunable pore structures, diverse functionalities, and high stability. Micro- and mesoporous polymers, in particular, have proven their feasibility in applications to storage, separation, and catalysis.[21] In catalytic applications, the rigid and chemically designable scaffolds of porous frameworks offer a reaction space suitable to molecular conversion in variety of reaction systems. The following section provides a summary of the continuous-flow application of phosphine-containing micro- and mesoporous polymers to transition-metal catalysis.
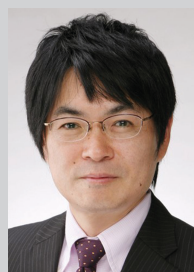
Hikaru Matsumoto received his Ph.D. degree (2021) from Kyushu University under the supervision of Professor Yoshiko Miura. He has been an Assistant Professor at Kyushu University since 2023. His research interest is on polymer-supported catalysts for synthesis of fine chemicals.

Yoshiko Miura received her Ph.D. degree (2000) from Kyoto University under the supervision of Professor Yukio Imanishi. She spent 1 year as a postdoctoral researcher at the University of Pennsylvania in Professor Virgil Percec's group (2000–2001). In 2001, she transferred to Nagoya University as an Assistant Professor. In 2005, she was appointed as an Associate Professor at Japan Advanced Institute of Science and Technology. In 2010, she was appointed as a Professor at Kyushu University. Her current research focuses on biopolymers based on precise polymer synthesis, and the development of new organic synthesis based on materials science.

Tomohiro Iwai received his Ph.D. degree (2011) from Kyoto University under the supervision of Professor Yasushi Tsuji. In 2011, he was appointed as an assistant professor at Hokkaido University. In 2020, he transferred to The University of Tokyo as a Lecturer. His research interest is on the development of highly efficient metal catalysis based on ligand design.

Masaya Sawamura received his Ph.D. degree (1989) from Kyoto University under the supervision of Professor Yoshihiko Ito. In 1989, he became Assistant Professor at Kyoto University. He spent one year as a researcher at Harvard University (1993–1994). In 1995, he transferred to Tokyo Institute of Technology and to the University of Tokyo. He was promoted to Lecturer in 1996 and to Associate Professor in 1997. Since 2001, he has been a Professor at Hokkaido University and a PI at the Institute of Chemical Reaction Design and Discovery, a part of the World Premier International Research Center Initiative (WPI-ICReDD).

ChemPlusChem

Review
doi.org/10.1002/cplu.202400039

Chemistry Europe
European Chemical
Societies Publishing

2.1. MOFs

For decades, coordination polymers have held a place in the realm of chemistry. A significant stride in coordination polymer chemistry has been achieved through the development of thermally stable porous coordination polymers (PCPs). Among them, MOFs have emerged as valuable materials with diverse applications, including gas storage,[22] separation,[23] sensing,[24] drug delivery,[25] and catalysis.[26] MOFs feature an open framework where inorganic clusters or isolated metal ions are bridged by organic ligands, creating a permanent microporosity. The choice of metal and ligand species allows for the creation of a variety of pore structure, providing control over pore size and volume. The microporous reaction space with tunable pore size proves highly attractive for enhancing selectivity in catalytic reactions. Due to their structural and chemical versatilities, stabilities, and excellent microporosities, MOF catalysts have demonstrated superior catalytic performance compared to their homogeneous counterparts.[27]

Redondo and co-workers reported a Ru-catalyzed dehydrogenation of formic acid under continuous-flow conditions (Figure 2).[28] They employed a phosphine-containing MOF (**LSK-15**) with a formulation of $[Al_3O(Cl,OH)(NH_2-C_8H_3O_4)_{2.64}(PPh_2-C_8H_3O_4)_{0.36}]_n$, originally developed by the authors.[29] Formic acid is considered an ideal H_2 source and H_2-storage material due to its high hydrogen content of 53 g-H_2 L^{-1} (or 4.4 wt%). The selective catalysis of decarboxylation (formation of H_2 and CO_2) over decarbonylation (formation of H_2O and CO) is crucial for efficient H_2 utilization.[30] Numerous studies on formic acid decomposition via decarboxylation using both homogeneous[31] and immobilized[32] catalysts have been reported. Ru was supported on the **LSK-15** by loading of $[Ru(p\text{-}cym)Cl_2]_2$ to form Ru-supported **LSK-15** (Ru-**LSK-15**). The **LSK-15** maintained its crystalline structure upon the Ru loading while decreasing its pore volume from 1.26 to 0.6 $cm^3 g^{-1}$, which indicated the incorporation of Ru complex inside the cage of **LSK-15**. The dehydrogenation of formic acid was performed using a fixed bed of Ru-**LSK-15** in a column reactor. Optimizing the reactor temperature, the Ru-**LSK-15** exhibited excellent activity (88±8% formic acid conversion, 2400±580 h^{-1} turnover frequency (TOF)) and selectivity to H_2 over CO (>99%). In a long-term

experiment of vapor-phase formic acid decomposition, the Ru-**LSK-15** demonstrated a constant TOF (2300±570 h^{-1}) and achieved a high turnover number (TON) (1290 000) without measurable deactivation over 23 days at 145°C. Transmission electron microscopy (TEM) analysis of the spent Ru-**LSK-15** showed no aggregation of supported Ru even after 23 days of continuous-flow operation, suggesting the effective prevention of Ru aggregation through strong coordination of phosphine within the micropores.

Another successful application of MOF catalyst to a continuous-flow synthesis was reported by Rimoldi and co-workers (Figure 3).[33] They chose **NU-1000**, composed of Zr_6 oxide metal nodes and 1,3,6,8,–tetrakis(*p*-benzoic acid)pyrene as tetratopic linkers, to form a mesoporous network with 30 Å channels. This MOF served as the scaffold for supporting bis-phosphinite-Ir pincer complex (Ir-**NU-1000**). Typically, the direct incorporation of a phosphine moiety into a MOF may lead to partial oxidation during synthesis, resulting in deterioration of well-defined coordination sites for complexation with metal catalysts.[34] To address this issue, the authors employed a solvent assisted ligand-incorporation (SALI), a post-synthetic functionalization method, for the preparation of Ir-**NU-1000**. ^{31}P solid-state nuclear magnetic resonance spectroscopy (SS NMR) confirmed that the successful incorporation of the carboxylic-acid-functionalized pincer complex into the MOF. The resulting Ir-**NU-1000** was evaluated for its catalytic activity and compared with a homogeneous Ir pincer complex in the hydrogenation of 1-decene and styrene. Under batch conditions, the TOFs of Ir-**NU-1000** were 2.3 h and 7.2 h^{-1} for the conversions of 1-decene and styrene, respectively, which were significantly higher than those of the homogeneous system (0.3 and 0.1 h^{-1}, respectively). Moreover, no detectable leaching of the supported Ir occurred in the reaction mixture, suggesting the strong chelation of Ir by the bis-phosphinite pincer ligand. The applicability of Ir-**NU-1000** to continuous-flow hydrogenation was confirmed using a fixed-bed reactor. The Ir-**NU-1000** was mixed with silica and deposited in a tubular reactor over a layer of quartz wool, and employed for gas-phase ethene hydrogenation under continuous-flow conditions. The TOF was 0.32 s^{-1} at 50°C, 1 bar (rel.) total gas pressure (ethene/H_2 1:1). At 23°C and 0.5 bar (rel.) total gas pressure, the continuous-
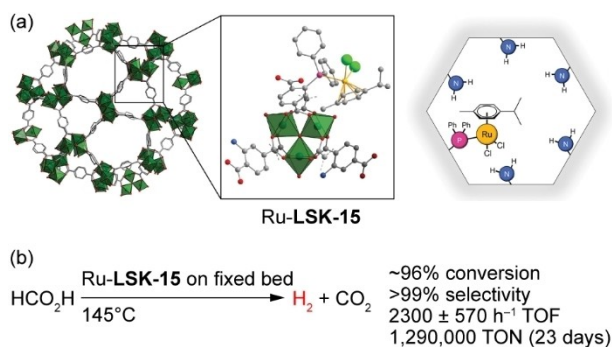

Figure 2. (a) MOF containing monophosphine-Ru complex (Ru-**LSK-15**) and (b) dehydrogenation of formic acid with the fixed bed of Ru-**LSK-15** in continuous-flow system. Adapted with permission from reference [28]. Copyright 2015 American Chemical Society.
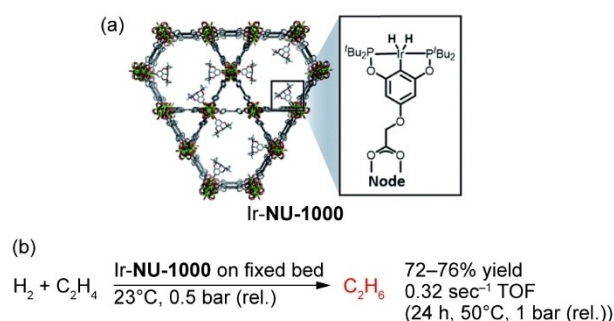

Figure 3. (a) MOF containinig bis-phosphinite-Ir pincer complex (Ir-**NU-1000**) and (b) hydrogenation of ethene with the fixed bed of Ir-**NU-1000** in continuous-flow system. Adapted with permission from reference [33]. Copyright 2016 The Royal Society of Chemistry.

ChemPlusChem

Review
doi.org/10.1002/cplu.202400039

Chemistry Europe
European Chemical
Societies Publishing

flow reactor of Ir-**NU-1000** was durable over 24 h on stream and showed minor losses of activity (only 4%).

Despite the feasibility of MOFs for immobilized catalysis, the transition from batch to continuous-flow systems remains limited. The inherent challenge arises from the typical formation of MOFs in polycrystalline powder, leading to difficulties in processing and handling within continuous-flow setups. This issue results in potential pressure drops, reactor clogging, and complicated recovery procedures. Addressing these challenges necessitates the formation and shaping of MOF catalysts into suitable forms, which is a task that is not easily accomplished.[35]

2.2. POPs

In the past decade, POPs have emerged as focal points in the field of catalytic chemistry due to their large surface area, controllable pore size, and high chemical durability. The POPs are amorphous polymers, extensively and covalently cross-linked, and primarily composed of C, O, N, and P. The porous polymer backbone of the POPs allows the integration of organic functional ligands, supporting transition-metal complexes for diverse catalytic applications.[36] Consequently, POPs featuring a broad range of phosphine moieties have spurred the development of polymer-supported phosphine-metal complexes, including Pd, Ir, Rh, and Ru complex.

Gunasekar and co-workers developed a bisphosphine-Ru complex supported on POP for the continuous-flow conversion of CO_2 into N,N-dimethylformamide (DMF) through hydrogenation (Figure 4).[37] The synthesis involved the conjugation of tetrakis(4-bromophenyl)methane and 1,2-bis(dichlorophosphino)ethane, followed by metalation with a methanolic solution of $RuCl_3$, resulting in a Ru-coordinated POP (Ru-**POP-BP**). The Ru-**POP-BP** catalyst featured a structure comprising micro- and mesopores (9.7 nm mean pore size) and a 469 $m^2 g^{-1}$ Brunauer–Emmett–Teller (BET) surface area. For continuous-flow CO_2 hydrogenation, a specially designed trickle-bed reactor system was employed. A Trickle-bed reactor is one of fixed-bed reactors where liquid and gas phases concurrently flow through a fixed bed of catalysts,[38] and has
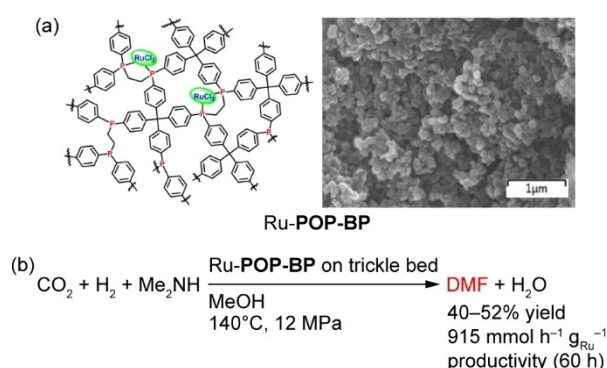
been widely used in chemical manufacturing of not only traditional petrochemicals but also biochemicals and fine chemicals.[39] The reactor system offers advantages in terms of mixing, heat transfer, scalability, energy efficiency, and sustainability during the continuous-flow processes. Remarkably, the Ru-**POP-BP** catalysts exhibited unprecedented activity in both batch (29,000 h^{-1} initial TOF and 160,000 TON) and continuous-flow processes (915 $mmol\,h^{-1}$ productivity per gram of Ru, 60 h on stream). The catalytic efficacy remained stable through successive runs in the batch system and durable over a long-term operation in the continuous-flow system.

In industrial processes, the hydroformylation of olefins stands out as a crucial homogeneous catalysis for synthesizing aldehydes and alcohols (ca. 10.4 million metric ton $year^{-1}$).[40] To achieve stable and recyclable catalysts for hydroformylations, extensive investigations have explored the use of porous materials.[41] Phosphine- or phosphite-Rh complexes are renowned catalysts for efficient and selective hydroformylation,[42] and efforts have been made to immobilize the complexes on POPs.[43] Jiang and co-workers demonstrated the effectiveness of three-fold cross-linking triphenylphosphine polymers in providing excellent catalytic activity and durability under continuous-flow Rh-catalyzed hydroformylation (Figure 5).[44] The POP with a triphenylphosphine moiety (**POP-TPP**) has been previously synthesized,[45] utilizing a three-fold vinylated triphenylphosphine polymerized in an autoclave under solvothermal condition. Serving as both support materials and ligands, the **POP-TPP** featured large surface area and pore volume of 1086 $m^2 g^{-1}$ and 1.70 $cm^3 g^{-1}$, respectively. In the continuous-flow hydroformylation of ethylene catalyzed by Rh-supported **POP-TPP** (Rh-**POP-TPP**) within a fixed-bed reactor, Rh-**POP-TPP** with a 0.125 wt% Rh loading achieved a 96.2% conversion of ethylene and a 96.1% selectivity for propanal at 120 °C and 1.0 MPa total pressure (ethylene/CO/H$_2$=1:1:1). Notably, the Rh-**POP-TPP** exhibited a higher TOF (4530 h^{-1}) than those of SiO_2-supported $Rh(CO)_2(acac)$ and $HRh(CO)(PPh_3)_3$ (30 and 1091 h^{-1} TOF, respectively). The authors attributed the superior

Figure 4. (a) POP containing bisphosphine-Ru complex (Ru-**POP-BP**) and (b) hydrogenation of CO_2 with the trickle bed of **Ru-POP-BP** in continuous-flow system. Adapted with permission from reference [37]. Copyright 2020 Wiley-VCH GmbH, Weinheim.
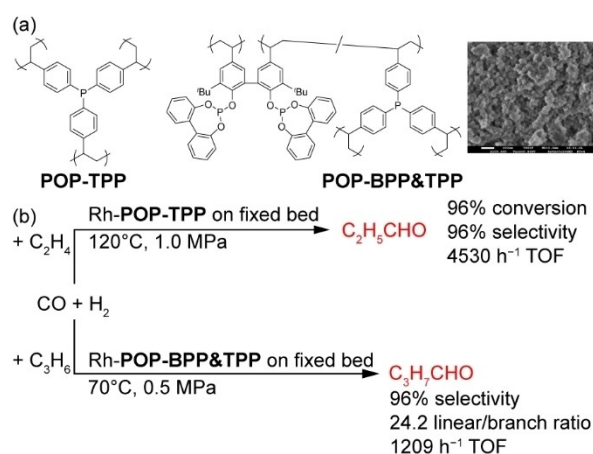
Figure 5. (a) POPs containing monophosphine (**POP-TPP**) and mono/bisphosphite (**POP-BPP&TPP**), and (b) hydroformylations with the fixed beds of Rh-supported POPs in continuous-flow system. Adapted with permission from reference [44]. Copyright 2015 Elsevier. Adapted with permission from reference [46]. Copyright 2016 The Royal Society of Chemistry.

ChemPlusChem

Review
doi.org/10.1002/cplu.202400039

Chemistry Europe
European Chemical
Societies Publishing

catalytic efficiency of the Rh-**POP-TPP** to the dual role of **POP-TPP** matrix as both support materials and ligands. The hierarchical porosity of the **POP-TPP** was suggested to facilitate full access of Rh molecules to the pore surface decorated with triphenylphosphine for complexation. The dispersion of single Rh atoms within the Rh-**POP-TPP** was confirmed by high-angle annular dark-field scanning transmission electron microscopy (HAADF-STEM), K-edge X-ray absorption fine structure (EXAFS), and extended X-ray absorption fine structure (XANES).

Li and co-workers developed a series of phosphine-containing POPs where BiPhePhos and triphenylphosphine were cross-linked within the same scaffold for continuous-flow hydroformylations (Figure 5).[46] By copolymerizing the two-fold vinylated BiPhePhos with tris(4-vinylphenyl)phosphane under solvothermal conditions, a POP containing dual phosphine ligands (**POP-BPP&TPP**) was successfully obtained. The resulting POP exhibited a synergistic effect for high regioselectivity and stability in Rh-catalyzed hydroformylation. A Rh-supported **POP-BPP&TPP** (Rh-P**OP-BPP&TPP**) was prepared by impregnating the **POP-BPP&TPP** with a THF solution of Rh(CO)$_2$(acac). Rh-**POP-BPP&TPP** (BiPhePhos and triphenylphosphine ratio of 1:10 w/w) showed large BET surface area (1059 m^{2}g^{-1}) and pore volume (2.32 cm^{3}g^{-1}), almost identical to those of the original **POP-BPP&TPP**. Coordination between the P atom and Rh was confirmed using ^{31}P SS NMR, EXAFS, and XPS characterizations of the Rh-**POP-BPP&TPP**. Rh K-edge k^3-weighted Fourier transform spectra from EXAFS revealed that Rh was dispersed as a single atom on the POP and coordinated by approximately one Biphephos and one triphenylphosphine for each Rh. For continuous-flow hydroformylation, the Rh-**POP-BPP&TPP** was packed in a column reactor (40 cm length and 9 mm inner diameter) with a filling material (quartz sand and silica wool). The catalytic performance was evaluated in the hydroformylation of propene at 70 °C and 0.5 MPa total pressure (propene/CO/H$_2$ 1:1:1). The Rh-**POP-BPP&TPP** showed better TOF (1209.0 h^{-1}) and selectivity (93.0% aldehyde yield, 24.2 linear to branched aldehyde (*l/b*) ratio) than those of Rh-supported BiphePhos on SiO$_2$ catalyst (356.3 h^{-1} TOF, 86.1% aldehyde yield, and 15.6 *l/b* ratio). Interestingly, increasing the incorporation ratio of BiphePhos to triphenylphosphine moiety (from 1:10 to 3:10 w/w) drastically enhanced TOFs (from 1100 to 1500 h^{-1}) and *l/b* ratio (from 21.5 to 29.6) and further increment of BiphePhos ratio deteriorated the TOF due to decreased accessibility into pore surface. It is noteworthy that any leaching of Rh in the eluent from the reactor was not detected, and the supported Rh did not aggregate to form nanoparticle on the Rh-**POP-BPP&TPP** during 1000 h on stream. The durability of the Rh-**POP-BPP&TPP** suggested the strong multi-coordination from BiphePhos and triphenylphosphine within the porous network. The same research group also reported detailed studies on the synergistic effect of **POP-BPP&TPP** in terms of chemical structure of phosphine ligands as cross-linkers.[47]

Recently, the regioselective hydrogenation of α,β-unsaturated aldehyde to unsaturated alcohol has attracted great interests in fine chemicals synthesis. In particular, the hydrogenation of cinnamaldehyde (CAL) is valuable for the synthesis of drugs, flavors, and perfumes.[48] Much attention has been paid to Ru-phosphine complex because of the relatively low cost of Ru among platinum group metals,[49] and immobilized catalysts supporting the Rh complex have been reported.[50] Chen and co-workers reported a Ru-catalyzed regioselective hydrogenation by the combination of Ru-supported **POP-TPP** (Ru-**POP-TPP**) and a continuous-flow reactor (Figure 6).[51] Impregnation of **POP-TPP** in a MeOH solution of RuCl$_3$ afforded Ru-**POP-TPP**, where micro- and mesoporosity was maintained, and coordination between Ru and P was confirmed using X-ray photoelectron spectroscopy (XPS) and ^{31}P SS NMR. The resulting Ru-**POP-TPP** was applied to heterogeneous and regioselective hydrogenation of CAL in a continuous-flow system using a trickle-bed reactor. The Ru-**POP-TPP** (40 cm length and 6 mm inner diameter) was set up, and CAL solution in a ^{t}BuOH/H$_2$O mixture (22:3 v/v) and H$_2$ were concurrently fed from the top of the reactor and flowed downward at 50 °C and 5.0 MPa. Compared with ZSM-35, activated carbon, and SiO$_2$, **POP-TPP** showed the highest performance in supporting Ru at the initial stage during the continuous-flow hydrogenation of CAL. It was found that the selectivity of Ru-**POP-TPP** for the conversion of CAL into cinnamyl alcohol (COL), hydrocinnamaldehyde (HCAL), and hydrocinnamyl alcohol (HCOL) was significantly dependent on the reaction temperature and H$_2$ pressure. The long-term durability of the Ru-**POP-TPP** was tested in the continuous-flow hydrogenation of CAL over 312 h on stream. The stable conversion of CAL (55%) and selectivity to COL (63%) were provided without leaching and aggregation of Ru catalysts.

The hydrosilylation of alkynes has attracted much interests due to its high efficiency and atom economy for vinylsilanes, which are crucial intermediates in organic syntheses.[52] For selective alkyne hydrosilylation, transition-metal catalysts containing precious metals such as Pt,[53] Rh,[54] Ru,[55] and Pd[56] have been employed. Recently, several groups have focused on developing selective hydrosilylation of alkynes using non-precious metal catalysts in the presence of well-designed homogeneous ligands.[57] Zhou and co-workers achieved the hydrosilylation of alkynes using Xantphos-Ni complex supported on POP with good reusability (Figure 7).[58] Four-fold cross-linking
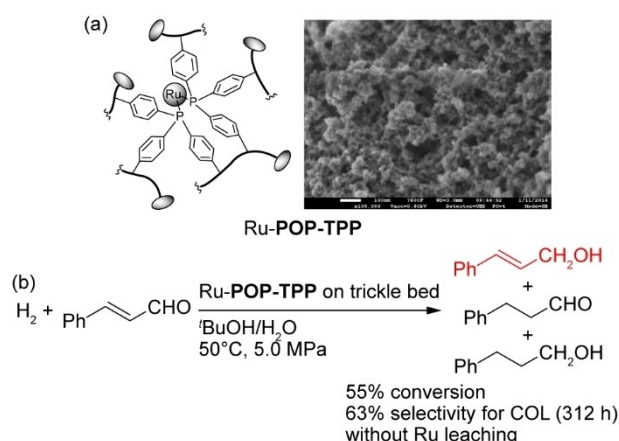

Figure 6. (a) POP containing phosphine-Ru complex (Ru-**POP-TPP**) and (b) hydrogenation of CAL with the trickle bed of Ru-**POP-TPP** in continuous-flow system. Adapted with permission from reference [51]. Copyright 2017 Springer Nature.
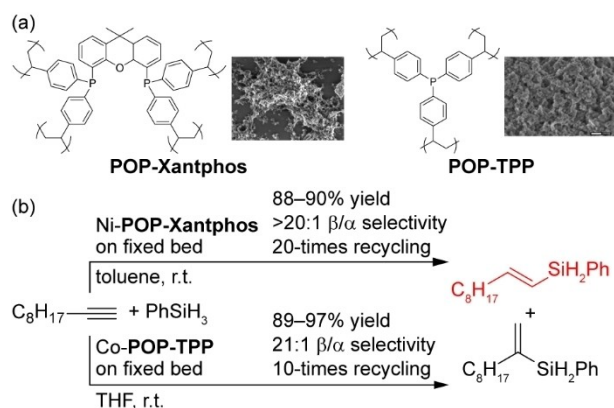
ChemPlusChem

Review
doi.org/10.1002/cplu.202400039

**Chemistry
Europe**
European Chemical
Societies Publishing

Figure 7. (a) POP containing Xantphos (**POP-Xantphos**) and **POP-TPP**, and (b) hydrosilylation of 1-decyne with the fixed beds of Ni- or Co-supported POPs in continuous-flow system. Adapted with permissions from references [58,59]. Copyright 2018 American Chemical Society.

Xantphos produced heterogeneous POP (**POP-Xantphos**), which had a hierarchical size of micropores (0.6 and 2.9 nm calculated by N_2 adsorption–desorption isotherms and nonlocal density functional theory (NLDFT)) and a large BET surface area (543 $m^2 g^{-1}$). Due to the microporous structure, the interaction between substrates and active sites were beneficial for boosting the efficiency and selectivity of hydrosilylation. Indeed, the Ni-supported **POP-Xantphos** (Ni-**POP-Xantphos**) showed better β/α (22:1) and E/Z ($> 20:1$) selectivities and yield (92%) for the hydrosilylation of 1-decyne with Ph_2SiH_2 than those of homogeneous mono- and bisphosphine counterparts (up to 60% yield) in the batch system. From the viewpoint of sensitivity to air and reusability of the Ni-**POP-Xantphos**, a continuous-flow reactor was constructed by charging a glass column with a mixture of the catalyst and sea sand. The continuous permeation of 1-decyne and $PhSiH_3$ in toluene through the column gave a comparable yield (89%) and β/α selectivity (21:1) with those in the batch system, and the catalytic durability was maintained during 10-times use in the continuous-flow system.

Regarding different transition-metal catalysis, the same research group also developed Co-catalyzed hydrosilylation using **POP-TPP** as a support (Figure 7).[59] Similar to the aforementioned Ni system, the Co-supported **POP-TPP** (Co-**POP-TPP**) successfully catalyzed the continuous-flow hydrosilylation of 1-decyne or phenylacetylene using a fixed-bed reactor. The continuous-flow reactor of Co-**POP-TPP** could be recycled at least 20 times, though periodic reloading of Co was necessary due to the loss of Co loading through dissociation of Co and triphenylphosphine.

3. Macroporous Polymers

Macroporous polymers are classical and common supports that have been investigated since the late 1950s for the production of ion-exchange resins with improved mechanical durability and faster diffusion kinetics.[60] The use of macorporous polymers in a continuous-flow system includes the simple preparation of a column reactor, facile control of surface chemistry, easy handling, and low pressure loss, which are quite beneficial for efficient and sustainable chemical manufacturing from bulk chemicals to fine chemicals.[61] Macroporous polymers are characterized by interconnected and micro-sized aggregates segregated by pores, providing structural rigidity through extensive crosslinking. Comparing with fine particulates of MOFs, COFs, and POPs, macroporous polymers can be easily obtained as regularly sized and spherical beads or monolithic rods with size-controlled flow-through macropores. Thus, they have higher permeability and more uniform permeation of feed through their column reactors than those of micro- and mesoporous polymers.[6] Indeed, these unique properties of macroporous polymers in continuous-flow applications have been widely utilized for not only ion-exchange,[62] but also recovery,[63] chromatography,[64] diagnostics,[65] solid-phase synthesis,[66] and catalysis.[67] In the following section, metal-phosphine complex supported on macroporous polymers for continuous-flow catalysis will be discussed.

3.1. Polymer Beads

Macroporous and spherical polymer beads can be prepared through suspension polymerization, similar to their gel-type counterparts. In this process, a monomer solution containing a cross-linker and an initiator (dispersion phase) is stirred in an aqueous medium (continuous phase). The monomer droplets, dispersed in a porogenic solvent and stabilized, undergo thermal initiation of polymerization until monomer consumption is complete, resulting in micro-sized and spherical beads. Various parameters, such as the size or shape of reactor and stirrer, stirring rate, volume ratio of the continuous and dispersion phases, concentration of stabilizer and porogenic solvent, and so on, are adjusted to control bead size and porosity. Porogens are typically unreactive during the polymerization and selected from poor- or nonsolvents of the produced polymers, as well as soluble linear polymers. After polymerization, unreacted monomers and residual solvents are removed by washing to obtain a macroporous architecture.[68] The surface chemistry of these beads can be functionally tailored through the direct incorporation of functional monomers or post-functionalization techniques.[69] These characteristics make such polymeric support suitable for efficient immobilized catalysts containing phosphine-metal complexes.

De Munck and co-workers developed a Rh-phosphine catalyst supported on macroporous polystyrene beads for the continuous-flow hydroformylation of propylene.[70] They used a commercial macroporous resin, Amberlite XAD-2 (particle size of 0.1–1.0 mm), and functionalized it through chloromethylation and subsequent phosphination at unreacted and residual double bonds in the polymer scaffold to achieve a single-point grafting diphenylphosphine (**PS-g-DPP**). The post-functionalization of the XAD-2 led to a reduction in BET surface areas (345, 284, and 168 $m^2 g^{-1}$ for fresh, chloromethylation, and phosphination) due to filling in intraparticle pores. The resulting **PS-g-DPP** was treated with a $[RhH(CO)(PPh_3)_3]$ solution in toluene to

ChemPlusChem

Review
doi.org/10.1002/cplu.202400039

Chemistry Europe
European Chemical
Societies Publishing

form Rh-phosphine catalyst (Rh-**PS-*g*-DPP**). Laser Raman spectroscopy and EXAFS measurements confirmed the successful incorporation of the diphenylphoshine moiety into the polymeric surface and its complexation with one anchored ligand, respectively. The catalytic performance in the gas-phase hydroformylation of propylene was evaluated under continuous-flow conditions at up to 140°C and 0.1 MPa total pressure. A fixed bed reactor was prepared using a glass column (15 cm length and 1 cm inner diameter) packed with the Rh-**PS-*g*-DPP** and glass wool as a catalyst and plug, respectively. Compared with a supported liquid phase catalyst (SLP-catalyst, 0.42–0.50 mm particle size) previously reported,[71] the Rh-**PS-*g*-DPP** exhibited a 2- to 5-fold higher production rate of butyraldehyde per Rh loading during 135 h on stream. The fast kinetics and fully accessible surface area of Rh-**PS-*g*-DPP** were advantageous over the limited boundary area between the liquid phase (reactive phase) and gas phase on the SLP-catalyst. Interestingly, the final productivity and selectivity of hydroformylation had trade-off relationships with diphenylphoshine moiety coverage on the polymer, suggesting the importance of the number of diphenylphoshine moieties available for ideal coordination with Rh.

Carlu and Caze reported a Ni-catalyzed dimerization of ethylene using macroporous polystyrene beads as support in a continuous-flow system.[72] They prepared single-point grafting triphenylphosphine on polystyrene beads (**PS-*g*-TPP**) through suspension polymerization in the presence of a diluent as a porogen (hexane or linear polystyrene), anchoring of Br groups, and subsequent phosphination. The polymer ligand was treated with $NiCl_2$ and $Al(C_2H_5)_2Cl$ as metal source and reductant, respectively, to form the immobilized catalyst (Ni-**PS-*g*-TPP**), with its homogeneous counterpart known as an efficient catalyst for the dimerization and oligomerization of olefins.[73] The pore volume (0.09–1.06 $cm^3 g^{-1}$) and surface area (5–238 $m^2 g^{-1}$) of the Ni-**PS-*g*-TPP** were determined using Hg intrusion porosimetry and N_2 adsorption/desorption tests, revealing different morphologies of the Ni-**PS-*g*-TPP** depending on the feed ratio of divinylbenzene and porogen, and types of porogen. When hexane was used as the porogen, large agglomerates of microspheres were formulated in the polymer beads, and hierarchical pores could be observed from meso- to macropores (ranging from 5–15 nm to 50–1000 nm pore diameters). The Ni-**PS-*g*-TPP** was evaluated under continuous-flow dimerization of ethylene using a tubular reactor. All the catalysts showed that the TOF based on the consumption of ethylene decreased while selectivity in butene formation remained. For a set of Ni-**PS-*g*-TPP** derived from hexane as the porogen, increasing surface area improved the TOF, although selectivity decreased due to oligomerization and isomerization. The undesired decrease in the catalytic activity of Ni-**PS-*g*-TPP** suggested a gradual coverage of the active surface on porous architecture due to blocking by condensed oligomers, supported by a lower pore volume of the spent Ni-**PS-*g*-TPP** than that of the fresh catalyst.

Andersson and Nikitidis demonstrated the potential of macroporous poly(trimethylolpropanetrimethacrylate) (PTRIM) beads in post-functionalization with a phosphinating reagent, coordination with Rh, and continuous-flow catalytic hydro-

formylation (Figure 8).[74] The PTRIM beads can be obtained by suspension or microsuspension polymerization using a porogenic mixture of toluene/isooctane, and contain unreacted and easily accessible double bonds (methacrylic groups). The residual double bonds on the PTRIM beads were available for functionalization by radical copolymerization (up to 40 wt% in the case of a chiral monomer).[75] Triphenylphosphine moiety was grafted to the PTRIM beads through the polymerization of acryloyl chloride followed by a reaction with *N*-methyl-4-(diphenylphosphino)benzylamine, providing **PTRIM-*g*-TPP**. The phosphine-containing **PTRIM-*g*-TPP** was treated with Rh-$(CO)_2$(acac) in dichloromethane (DCM) to form Rh-phosphine supported **PTRIM-*g*-TPP** (Rh-**PTRIM-*g*-TPP**). 1-Hexene saturated with H_2 and CO was permeated through the fixed bed of Rh-**PTRIM-*g*-TPP** in a tubular reactor. The initial activity of Rh-**PTRIM-*g*-TPP** showed a rather high yield of aldehyde (up to 87%), which gradually attenuated under all the reaction conditions (different temperature and total pressure) while regioselectivity did not change significantly. The "burst" of catalytic activity at the initial stage suggested the generation of active species via oxidative addition of H_2 and reductive elimination of acetylacetone. The author mentioned that the resulting mono-ligating phosphine complex was highly active in hydroformylation over bis-ligating phosphine complex, and their equilibria could be controlled by reaction temperature. In addition, dissolution of Rh from Rh-**PTRIM-*g*-TPP** (12–18% of the initial Rh loading) was implied, however, the decrease in catalytic activity was not directly explained by the loss of Rh loading.

As seen in the previous sections, continuous-flow applications of micro-, meso, and macroporous polymers often adopt packed-bed reactors because of their wide applicability and simple and on-site preparation by users. Nir and Pismen simulated a considerable improvement in the efficiency of the packed bed of macroporous catalyst, highlighting forced convection in intraparticle pores.[76] Regnier and co-workers used polymer beads with large flow-through pore diameters of 10 and 0.8 μm, and applied them to chromatography, diagnostic, and enzyme immobilizations, leading to improved separation efficiency of the packed-bed column.[77] However, convective flow around the particles was still favored, accounting
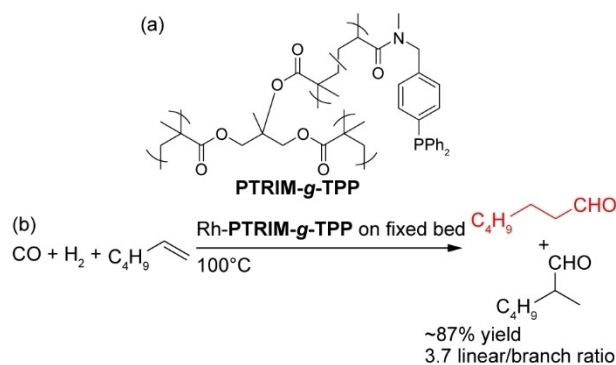

Figure 8. (a) Polymer beads containing monophosphine (**PTRIM-*g*-TPP**) and (b) hydroformylation of 1-hexene with the fixed bed of Rh-supported **PTRIM-*g*-TPP** in continuous-flow system.

ChemPlusChem

Review
doi.org/10.1002/cplu.202400039

Chemistry Europe
European Chemical
Societies Publishing

for 98% of the total convection flow (Figure 9a). Generally, fluid flows through interparticle voids where the flow resistance is minimum, while the fluid in the intraparticle pores remains stagnant. In this situation, it is challenging for substances to intimately contact the active sites in the intraparticle pores due to diffusion limitations, resulting in lower catalytic efficiency. Additionally, catalyst particles tend to be densely packed during continuous-flow processes, and interparticle voidage reaches as low as 36%.[78] This restricts the feasibility of finely powdered catalysts for continuous-flow reactors due to low permeability of substrate solutions. Thus, there is a clear demand to develop a column reactor that has both a narrow pore size distribution and high voidage for the full convection of substrates and high permeability.

3.2. Polymer Monolith

A monolith is defined as "a shaped, fabricated intractable article with a homogeneous microstructure that does not exhibit any structural components distinguishable by optical microscopy," according to IUPAC.[79] In modern continuous-flow applications, monolith is recognized as a single and self-standing material featuring interconnected and flow-through pores. In the early 1990s, Fréchet and Svec first introduced a monolith column based on a rigid macroporous polymer for continuous-flow applications.[80] The self-supporting nature, high porosity, and narrow pore size distribution of the monolith achieve fluid permeation at low pressure loss and narrow residence time distribution, leading to intimate contact between reactants and active sites. Thus, it overcomes the limitations of permeability and mass transfer in the polymer bead system (Figure 9b). These pioneering works have provided chemists with useful tools for fast, high-efficiency, and low-pressure-loss flow applications. The monolith can be produced by a simple "molding" process, typically using an empty column as the mold. The mold filled with a polymerization mixture is sealed at both ends, then heated for the initiation of bulk polymerization. In contrast to the suspension polymerization for macroporous polymer beads, the "stirring-free" process of bulk polymerization provides a single and rigid polymer within the mold, which can be directly utilized as a continuous-flow reactor.[81]

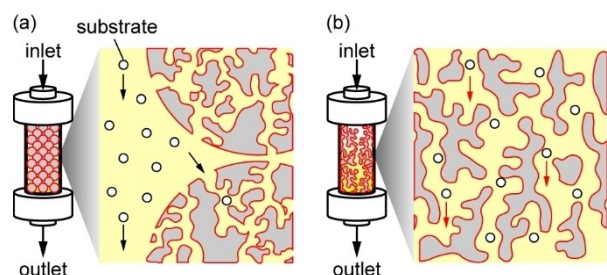The most common method to form the flow-through pores in the monolith is polymerization-induced phase separation (PIPS), which occurs during polymerization in the presence of a poor- or nonsolvent as a porogen (Figure 10a). In PIPS, key variables to tune the porous properties of monoliths include polymerization temperature and time, composition of the porogenic solvent, content of cross-linking monomer, and so on.[82] Another important and unique approach to pore formation is based on a high-internal phase emulsion (HIPE) system, which was first developed by Barby and Haq,[83] and extensively studied by Sherrington and Cameron.[84] The porosity of HIPE-based monoliths can be as high as 74~95% and is controlled by the volume ratio of the dispersion and continuous phases in the template emulsion, along with changes in pore structure (Figure 10b). In catalytic applications under continuous-flow conditions, monoliths are considered ideal candidates due to their simple preparation, high permeability, and controllable pore size distribution. Indeed, many studies on monolith reactors have demonstrated their feasibility in continuous-flow reactions catalyzed by transition metals such as Ir,[85] Pd,[86] and Ru.[87] The enhanced catalytic activities of the monoliths over those of polymer beads were attributed to the narrow residence time distributions.[86e]

Metathesis is recognized as one of the most important organic reactions for C—C bond formation and has seen significant advancements with catalytic systems based on organometallics, as observed in the elegant researches by Grubbs.[88] The importance of ring-opening metathesis polymerization (ROMP) and ring-closing metathesis (RCM) has been witnessed in the fields of polymer chemistry, pharmaceuticals, and combinatorial chemistry.[89] Buchmeiser's research group has proposed a novel concept for the derivatization of terminal groups on monoliths, involving the following steps: 1) the formation of a continuous and rigid monolith structure by ROMP under PIPS conditions, and 2) incorporation of functional monomers into the "living" terminal groups ligating the 1st
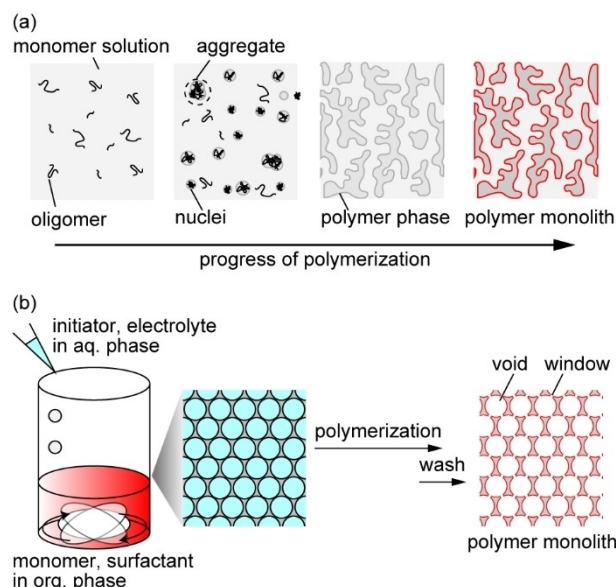

Figure 9. Schematic view of continuous-flow fluid in column employing (a) macroporous polymer beads and (b) polymer monolith.

Figure 10. Mechanism of pore formation via (a) PIPS and (b) water-in-oil HIPE template through radical polymerization.

ChemPlusChem

Review
doi.org/10.1002/cplu.202400039

Chemistry
Europe

European Chemical
Societies Publishing

generation Grubbs catalyst, which contains a phosphine-Ru complex formulated as [Cl$_2$(PR$_3$)$_2$–Ru(=CHPh)] (R=cyclohexyl, phenyl].[90] They recognized this ROMP-derived monolith with reactive termini as an immobilized Ru catalyst, and extended the concept to the heterogenization of the second 2nd generation Grubbs catalyst, which contains a Ru-phosphine-*N*-heterocyclic carbene (NHC) complex for continuous-flow ROMP and RCM (Figure 11).[91] The use of the NHC ligand effectively generated highly active Ru carbenes and enhanced the durability of the corresponding Ru-phosphane-NHC complex against Ru leaching. The ROMP-derived monolith was obtained through the copolymerization of norbornene and 1,4,4a,5,8,8a-hexahydro-1,4,5,8-*exo-endo*-dimethanonaphthalene in the presence of DCM and 2-propanol. Through the optimization of porous structures, a monolith with 1.5±0.5 μm microglobule diameter and 40% interparticle porosity was selected. Careful avoidance of micropore formation within the microglobules significantly enlarged the availability of Ru centers at polymer chain termini on the microglobule surface for the incorporation of the Ru-phosphine-NHC catalyst, despite its low surface area. The resulting Ru catalyst on the monolith exhibited high TOFs for RCM of dienes (up to 25 min^{-1} for diethyl diallylmalonate) and good *cis/trans* selectivity (10:90) for ROMP of norbornene or cyclooctene, comparable with those of the homogeneous counterpart. The grafting-from derivatization of the Ru-phosphine-NHC complex and the absence of microporosity reduced the diffusion-controlled regime in the catalytic processes, demonstrating excellent reactivities. Additionally, the coordination of the NHC ligand with the Ru center successfully minimized Ru leaching to below 70 ppm.[91] In a series of comparative studies on the catalytic efficiency of the Ru-phosphine-NHC complex on the monolith, Buchmeiser and co-workers also evaluated the packed bed of silica-supported Ru-phosphine-NHC complex for catalytic efficiency in continuous-
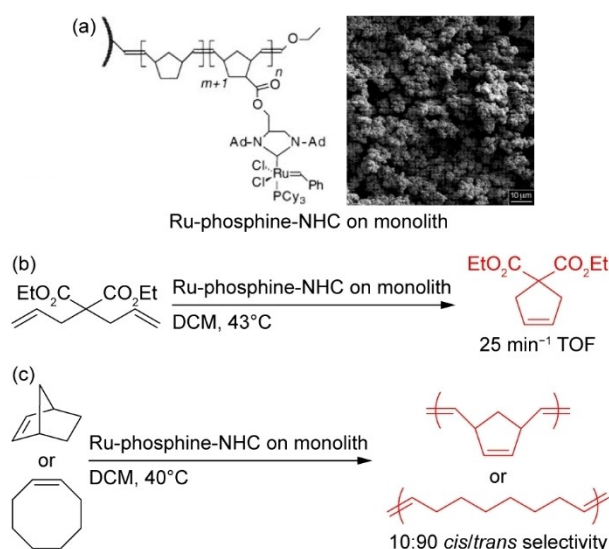
flow RCM of diethyl diallylmalonate.[91] Interestingly, lower activities (1–90 TONs) of the silica-based catalysts were observed than those of polymer monoliths (30–940 TONs), which might be attributed to both the non-reversible trapping of the phosphine ligand by free silanol groups[88] and diffusion-limited reactions in the microporous structure of silica supports. Obviously, the advantage of the chemically inert matrix and tunable porous properties of the ROMP-derived monoliths were highlighted.

C−C or C-heteroatom cross-couplings are powerful tools to produce pharmaceuticals or agricultural drugs. Advances in cross-couplings for a broad range of substrate scopes have been encouraged by the development of sophisticated organo-metallics, including phosphine-metal catalysts.[92] In continuous-flow cross-couplings using immobilized catalysts, the reactor should be carefully designed to avoid serious clogging by insoluble salt bases in organic solvent.[93] One solution was proposed by Naber and Buchwald, where an organic/aqueous biphasic solvent was used to deliver all the reactants smoothly through a continuous-flow reactor.[94] Under the biphasic reaction conditions, mixing of reactants is an important factor to maintain a large reaction interface within a catalytic column reactor. Our research group first reported a hybridization of a porous polymer monolith and phosphine-metal complex for better mixing of the biphasic reaction mixture and high-productivity continuous-flow synthesis (Figure 12).[95] Through radical copolymerization, a three-fold cross-linking triphenyl-phosphine was incorporated into a HIPE-based highly porous polystyrene monolith to provide an **M-PS-TPP**. Owing to three-fold cross-linking around the supported triphenylphosphine, the **M-PS-TPP** showed selective mono-coordination toward Pd over bis-coordination confirmed by ^{31}P SS NMR, which contrasted sharply with that of a monolith supporting a single-point grafting triphenylphosphine (**M-PS-*g*-TPP**). The pore size and porosity of the **M-PS-TPP** were up to 10.7 μm and 81%, determined by Hg intrusion porosimetry, which were high enough to allow fast permeation at low pressure loss. Indeed, the Darcy's permeabilities of the monolith columns were preferentially high (3.8×10^{-14}–3.3×10^{-13} m^2) and the residence

Figure 11. (a) ROMP-derived polymer monolith containing Ru-phosphine-NHC complex, (b) RCM of diethyl diallylmalonate, and (c) ROMP of norbornene or cyclooctene with the monolith reactor in continuous-flow system. Adapted with permission from reference [91a]. Copyright 2001 Wiley-VCH GmbH, Weinheim.
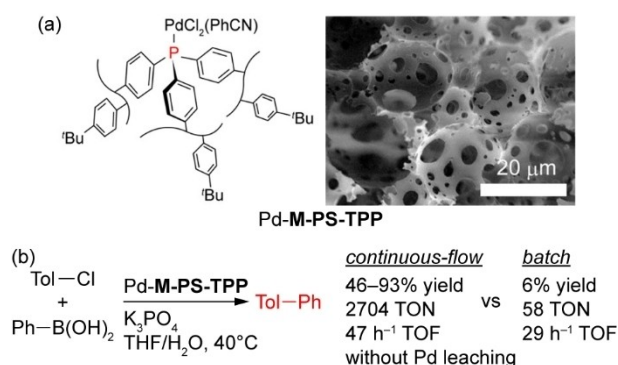

Figure 12. (a) Polystyrene monolith containing monophosphine-Pd complex (Pd-**M-PS-TPP**) and (b) cross-coupling between chlorotoluene and phenyl-boronic acid with the reactor Pd-**M-PS-TPP** in continuous-flow system. Adapted with permission from reference [95]. Copyright 2020 American Chemical Society.

ChemPlusChem

Review
doi.org/10.1002/cplu.202400039

**Chemistry
Europe**
European Chemical
Societies Publishing

time distribution of the column were quite narrow and close to an ideal plug flow. The unique ligand performance and hydrodynamic characteristics of the **M-PS-TPP** column were evaluated in the continuous-flow C—C cross-couplings of chlorotoluene and phenylboronic acid in THF/K_3PO_4 aq., which revealed the high TOFs and TONs of Pd-supported **M-PS-TPP** (Pd-**M-PS-TPP**) reactor over Pd-supported **M-PS-g-TPP** (Pd-**M-PS-g-TPP**) reactor. Noteworthy, the optimization of linear velocity of the feed mixture significantly improved yield (from 8 to 88%). At these optimized conditions, the use of a pre-mixer for the organic/aqueous feed and a phase transfer catalyst (tetrabutylammonium bromide) had little influence on the catalytic efficiency, which demonstrated that the diffusion limitation at the organic/aqueous phase interface was overcome using the Pd-**M-PS-TPP** reactor unlike homogeneous catalyst system.[94] The improvement of mass transfer was further highlighted in a comparative experiment, in which the Pd-**M-PS-TPP** column reached a much higher catalytic performance (47 h^{-1} TOF and 2704 TON, at 2.0 h residence time and 58 h on stream) than that of the batch system (29 h^{-1} TOF and 58 TON, at 2.0 h reaction time).

Very recently, we further carefully designed this **M-PS-TPP** system for further improved catalytic durability of the phosphine-metal complex based on polymer-metal interaction.[96] Our concept was inspired by a series of elegant researches on polymer-incarcerated (PI) catalysts of metal nanoparticles developed by Kobayashi and co-workers.[11] PI catalysts were stabilized via interactions between the π-electrons of phenyl rings on the polymer side chain and metal nanoparticles, and the electronic properties of the aromatic rings could influence the modulation of the stabilization, as suggested by Michaelis and co-workers.[97] Based on the sums of *para*-Hammett substituent constants ($\Sigma(\sigma_p)$), we screened styrene derivatives for modulation of electronic properties of aromatic rings on the hybrid monolith. A parent styrene (R=H) and its derivatives containing neutral (R=4-Ph), electron-donating (R=4-Me, 4-^{t}Bu, 4-OMe, 4-NMe$_2$), and electron-withdrawing substituents (R=4-F, 3,4,5-triF, 2,3,4,5,6-pentaF, 4-CF$_3$) were independently copolymerized with divinylbenzene and three-fold cross-linking triphenylphosphine. ^{31}P SS NMR confirmed no significant difference in selectivity for mono-P-ligation of the **M-PS-TPP**s. Scanning electron microscopy (SEM), Hg intrusion porosimetry, pulse-tracer experiments, and permeation tests also revealed little effects of styrene derivatives on the porous properties of the **M-PS-TPP**s. On the other hand, the incorporation of different styrene derivatives drastically influenced the TOFs and TONs of Pd-**M-PS-TPP**s in continuous-flow cross-couplings. Increasing electron-donating properties obtained higher TONs (1325–2911), while electron-withdrawing groups on styrene derivatives decreased the TONs (1038–1210). It was suggested that the electronic properties of styrene derivatives regulated the catalytic durability of Pd-**M-PS-TPP**s as follows: Pd^{II} pre-catalyst is coordinated to a labile ligand (PhCN or solvent) and triphenylphosphine on polystyrene. Subsequently, the aryl pendants on the polystyrene stabilize the triphenylphosphine-Pd complex via aromatic π-electron donations and/or coordination of functional groups on the aromatic

rings. The degree of the stabilization from the aryl pendants, that is, the production rate of catalytically active Pd^0 from the Pd^{II} pre-catalyst should be moderate for high catalytic durabilities.

4. Summary and Outlook

This review summarizes several continuous-flow reactor systems, highlighting the potential of phosphine-metal complexes supported on porous polymers. It is evident that microporous polymers such as MOFs and POPs offer great potential for transition-metal catalyst systems due to their flexible design of porous structures and ligands, enabling high surface area, controllable pore sizes, and single-site catalytic centers. However, challenges related to scalability for production and handling in continuous-flow processes still require significant improvement. On the other hand, macroporous polymers such as polymer beads and monoliths present several advantages in terms of scalability, reproducibility, controllability in the size of support. These advantages are ensured by established techniques in conventional polymerization systems and phase separation. By designing and fabricating catalytic systems that combine microporous networks with macroporous architectures, the resulting hierarchical porous structures have the potential to drive the development of useful, sustainable, and efficient immobilized catalysts for continuous-flow syntheses. This includes not only phosphine-metal complexes but also a broad range of organometallics for challenging organic transformations in the future.

Conflict of Interests

The authors declare no conflict of interest.

Keywords: continuous-flow reactions · immobilized catalysts · porous polymers · transition metals · phosphane ligands

[1] a) M. B. Plutschack, B. Pieber, K. Gilmore, P. H. Seeberger, *Chem. Rev.* **2017**, *117*, 11796–11893; b) J. Britton, C. L. Raston, *Chem. Soc. Rev.* **2017**, *46*, 1250–1271; c) S. R. Gobert, S. Kuhn, L. Braeken, L. C. Thomassen, *Org. Process Res. Dev.* **2017**, *21*, 531–542; d) A. Nagaki, *Tetrahedron Lett.* **2019**, *60*, 150923.

[2] C. W. Coley, D. A. Thomas III, J. A. M. Lummiss, J. N. Jaworski, C. P. Breen, V. Schultz, T. Hart, J. S. Fishman, L. Rogers, H. Gao, R. W. Hicklin, P. P. Plehiers, J. Byington, J. S. Piotti, W. H. Green, A. J. Hart, T. F. Jamison, K. F. Jensen, *Science* **2019**, *365*, eaax1566.

[3] a) A. Kirschning, W. Solodenko, K. Mennecke, *Chem. Eur. J.* **2006**, *12*, 5972–5990; b) S. Hübner, J. G. De Vries, V. Farina, *Adv. Synth. Catal.* **2016**, *358*, 3–25; c) K. Masuda, T. Ichitsuka, N. Koumura, K. Sato, S. Kobayashi, *Tetrahedron* **2018**, *74*, 1705–1730.

ChemPlusChem

Review

doi.org/10.1002/cplu.202400039

Chemistry Europe
European Chemical
Societies Publishing

[4] a) P. Kumar, A. Das, B. Maji, *Org. Biomol. Chem.* **2021**, *19*, 4174–4192; b) T. Drake, P. Ji, W. Lin, *Acc. Chem. Res.* **2018**, *51*, 2129–2138.

[5] K. S. W. Sing, D. H. Everett, R. A. W. Haul, L. Moscou, R. A. Pieroti, J. Rouquerol, T. Siemieniewska, *Pure Appl. Chem.* **1985**. *57*, 603–619.

[6] F. Svec, J. M. J. Frechet, *Science* **1996**, *273*, 205–211.

[7] a) V. Polshettiwar, C. Len, A. Fihri, *Coord. Chem. Rev.* **2009**, *253*, 2599–2626; b) P. W. N. M. Van Leeuwen, A. J. Sandee, J. N. H. Reek, P. C. J. Kamer, *J. Mol. Catal. A* **2002**, *182*, 107–123.

[8] a) N. E. Leadbeater, M. Marco, *Chem. Rev.* **2002**, *102*, 3217–3274; b) J. Lu, P. Toy, *Chem. Rev.* **2009**, *109*, 815–838.

[9] a) T. Yamamoto, M. Suginome, *Angew. Chem. Int. Ed.* **2009**, *48*, 539–542; b) T. Yamamoto, T. Yamada, Y. Nagata, M. Suginome, *J. Am. Chem. Soc.* **2010**, *132*, 7899–7901; c) T. Yamamoto, Y. Akai, Y. Nagata, M. Suginome, *Angew. Chem. Int. Ed.* **2011**, *50*, 8844–8847; d) Y. Akai, T. Yamamoto, Y. Nagata, T. Ohmura, M. Suginome, *J. Am. Chem. Soc.* **2012**, *134*, 11092–11095.

[10] a) T. Iwai, T. Harada, K. Hara, M. Sawamura, *Angew. Chem. Int. Ed.* **2013**, *52*, 12322–12326; b) T. Iwai, K. Asano, T. Harada, M. Sawamura, *Bull. Chem. Soc. Jpn.* **2017**, *90*, 943–949; c) T. Iwai, T. Harada, H. Shimada, K. Asano, M. Sawamura, *ACS Catal.* **2017**, *7*, 1681–1692; d) J. Arashima, T. Iwai, M. Sawamura, *Chem. Asian J.* **2019**, *14*, 411–415.

[11] a) S. Kobayashi, S. Nagayama, *J. Am. Chem. Soc.* **1998**, *120*, 2985–2986; b) R. Akiyama, S. Kobayashi, *Angew. Chem. Int. Ed.* **2001**, *40*, 3469–3471; c) R. Akiyama, S. Kobayashi, *J. Am. Chem. Soc.* **2003**, *125*, 3412–3413; d) K. Okamoto, R. Akiyama, S. Kobayashi, *Org. Lett.* **2004**, *6*, 1987–1990; e) K. Okamoto, R. Akiyama, S. Kobayashi, *Org. Lett.* **2005**, *7*, 4831–4834; f) H. Oyamada, R. Akiyama, H. Hagio, T. Naito, S. Kobayashi, *Chem. Commun.* **2006**, *41*, 4297–4299; g) H. Miyamura, R. Matsubara, Y. Miyazaki, S. Kobayashi, *Angew. Chem. Int. Ed.* **2007**, *46*, 4151–4154; h) H. Miyamura, M. Shiramizu, R. Matsubara, S. Kobayashi, *Angew. Chem. Int. Ed.* **2008**, *47*, 8093–8095; i) T. Yasukawa, H. Miyamura, S. Kobayashi, *J. Am. Chem. Soc.* **2012**, *134*, 16963–16966.

[12] C. Merckle, S. Haubrich, J. Blümel, *J. Organomet. Chem.* **2001**, *627*, 44–54.

[13] F. M. Rodrigues, R. M. Carrilho, M. M. Pereira, *Eur. J. Inorg. Chem.* **2021**, *2021*, 2294–2324.

[14] T. Matsumoto, M. Ueno, N. Wang, S. Kobayashi, *Chem. Asian J.* **2008**, *3*, 196–214.

[15] M. Pagliaro, V. Pandarus, R. Ciriminna, F. Béland, P. D. Carà, *ChemCatChem* **2012**, *4*, 432–445.

[16] A. Dewaele, F. Verpoort, B. Sels, *ChemCatChem* **2016**, *8*, 3010–3030.

[17] a) P. Gäumann, D. Cartagenova, M. Ranocchiari, *Eur. J. Org. Chem.* **2022**, *2022*, e202201006; b) G. R. Orton, B. S. Pilgrim, N. R. Champness, *Chem. Soc. Rev.* **2021**, *50*, 4411–4431.

[18] Q. Wang, D. Astruc, *Chem. Rev.* **2019**, *120*, 1438–1511.

[19] X. Guan, F. Chen, Q. Fang, S. Qiu, *Chem. Soc. Rev.* **2020**, *49*, 1357–1384.

[20] Y. Zhang, S. N. Riduan, *Chem. Soc. Rev.* **2012**, *41*, 2083–2094.

[21] a) Q. Sun, Z. Dai, X. Meng, F. S. Xiao, *Chem. Soc. Rev.* **2015**, *44*, 6018–6034; b) L. Tan, B. Tan, *Chem. Soc. Rev.* **2017**, *46*, 3322–3356; c) W. Zhang, H. Zuo, Z. Cheng, Y. Shi, Z. Guo, N. Meng, A. Thomas, Y. Liao, *Adv. Mater.* **2022**, *34*, 2104952.

[22] a) T. A. Makal, J. R. Li, W. Lu, H. C. Zhou, *Chem. Soc. Rev.* **2012**, *41*, 7761–7779; b) W. Fan, X. Zhang, Z. Kang, X. Liu, D. Sun, *Coord. Chem. Rev.* **2021**, *443*, 213968.

[23] a) C. Petit, *Curr. Opin. Chem. Eng.* **2018**, *20*, 132–142; b) M. F. Ghazvini, M. Vahedi, S. N. Nobar, F. Sabouri, *J. Environ. Chem. Eng.* **2021**, *9*, 104790.

[24] a) E. A. Dolgopolova, A. M. Rice, C. R. Martin, N. B. Shustova, *Chem. Soc. Rev.* **2018**, *47*, 4710–4728; b) B. Yan, *J. Mater. Chem. C* **2019**, *7*, 8155–8175.

[25] H. D. Lawson, S. P. Walton, C. Chan, *ACS Appl. Mater. Interfaces* **2021**, *13*, 7004–7020.

[26] a) J. Liu, T. A. Goetjen, Q. Wang, J. G. Knapp, M. C. Wasson, Y. Yang, Z. H. Syed, M. Delferro, J. M. Notestein, O. K. Farha, J. T. Hupp, *Chem. Soc. Rev.* **2022**, *51*, 1045–1097; b) Q. Wang, D. Astruc, *Chem. Rev.* **2019**, *120*, 1438–1511; c) H. Konnerth, B. M. Matsagar, S. S. Chen, M. H. Prechtl, F. K. Shieh, K. C. W. Wu, *Coord. Chem. Rev.* **2020**, *416*, 213319; d) M. Liu, J. Wu, H. Hou, *Chem. Eur. J.* **2019**, *25*, 2935–2948.

[27] D. Farrusseng, S. Aguado, C. Pinel, *Angew. Chem. Int. Ed.* **2009**, *48*, 7502–7513.

[28] A. B. Redondo, F. L. Morel, M. Ranocchiari, J. A. van Bokhoven, *ACS Catal.* **2015**, *5*, 7099–7103.

[29] a) F. L. Morel, M. Ranocchiari, J. A. van Bokhoven, *Ind. Eng. Chem. Res.* **2014**, *53*, 9120–9127; b) F. L. Morel, S. Pin, T. Huthwelker, M. Ranocchiari, J. A. van Bokhoven, *Phys. Chem. Chem. Phys.* **2015**, *17*, 3326–3331.

[30] W. Gan, P. J. Dyson, G. Laurenczy, *ChemCatChem* **2013**, *5*, 3124–3130.

[31] N. Onishi, R. Kanega, H. Kawanami, Y. Himeda, *Molecules* **2022**, *27*, 455.

[32] a) M. Ojeda, E. Iglesia, *Angew. Chem. Int. Ed.* **2009**, *48*, 4800–4803; b) K. Tedsree, T. Li, S. Jones, C. W. A. Chan, K. M. K. Yu, P. A. J. Bagot, E. A. Marquis, G. D. W. Smith, S. C. E. Tsang, *Nat. Nanotechnol.* **2011**, *6*, 302–307; c) Q. Y. Bi, X. L. Du, Y. M. Liu, Y. Cao, H. Y. He, K. N. Fan, *J. Am. Chem. Soc.* **2012**, *134*, 8926–8933.

[33] M. Rimoldi, A. Nakamura, N. A. Vermeulen, J. J. Henkelis, A. K. Blackburn, J. T. Hupp, J. F. Stoddart, O. K. Farha, *Chem. Sci.* **2016**, *7*, 4980–4984.

[34] X. Xu, S. M. Rummelt, F. L. Morel, M. Ranocchiari, J. A. van Bokhoven, *Chem. Eur. J.* **2014**, *20*, 15467–15472.

[35] B. Yeskendir, J. P. Dacquin, Y. Lorgouilloux, C. Courtois, S. Royer, J. Dhainaut, *Mater Adv* **2021**, *2*, 7139–7186.

[36] W. Wang, L. Cui, P. Sun, L. Shi, C. Yue, F. Li, *Chem. Rev.* **2018**, *118*, 9843–9929.

[37] G. H. Gunasekar, S. Padmanaban, K. Park, K. D. Jung, S. Yoon, *ChemSusChem* **2020**, *13*, 1735–1739.

[38] M. Herskowitz, J. M. Smith, *AIChE J.* **1983**, *29*, 1–18.

[39] a) M. Devarapalli, H. K. Atiyeh, J. R. Phillips, R. S. Lewis, R. L. Huhnke, *Bioresour. Technol.* **2016**, *209*, 56–65; b) T. Zhang, G. Yin, B. Li, X. Wang, S. Jiang, Z. Yuan, *Res. Chem. Intermed.* **2015**, *41*, 663–677.

[40] R. Franke, D. Selent, A. Börner, *Chem. Rev.* **2012**, *112*, 5675–5732.

[41] a) X. S. Zhao, X. Y. Bao, W. Guo, F. Y. Lee, *Mater. Today* **2006**, *9*, 32–39; b) C. Li, W. Wang, L. Yan, Y. Ding, *Front. Chem. Sci. Eng.* **2018**, *12*, 113–123.

[42] A. Corma, H. García, F. X. L. Xamena, *Chem. Rev.* **2010**, *110*, 4606–4655.

[43] a) Q. Sun, Z. Dai, X. Liu, N. Sheng, F. Deng, X. Meng, F. S. Xiao, *J. Am. Chem. Soc.* **2015**, *137*, 5204–5209; b) Q. Sun, Z. Dai, X. Meng, F. S. Xiao, *Catal. Today* **2017**, *298*, 40–45; c) Z. Liang, J. Chen, X. Chen, K. Zhang, J. Lv, H. Zhao, G. Zhang, C. Xie, L. Zong, X. Jia, *Chem. Commun.* **2019**, *55*, 13721–13724; d) M. Wu, G. Gao, C. Yang, P. Sun, F. Li, *J. Org. Chem.* **2022**, *88*, 5059–5068.

[44] M. Jiang, L. Yan, Y. Ding, Q. Sun, J. Liu, H. Zhu, R. Lin, F. Xiao, Z. Jiang, J. Liu, *J. Mol. Catal. A* **2015**, *404*, 211–217.

[45] Q. Sun, M. Jiang, Z. Shen, Y. Jin, S. Pan, L. Wang, X. Meng, W. Chen, Y. Ding, J. Li, F. S. Xiao, *Chem. Commun.* **2014**, *50*, 11844–11847.

[46] C. Li, L. Yan, L. Lu, K. Xiong, W. Wang, M. Jiang, J. Liu, X. Song, Z. Zhan, Y. Ding, *Green Chem.* **2016**, *18*, 2995–3005.

[47] a) Y. Wang, L. Yan, C. Li, M. Jiang, W. Wang, Y. Ding, *Appl. Catal. A* **2018**, *551*, 98–105; b) Y. Wang, M. Jiang, L. Yan, C. Li, G. Wang, W. He, Y. Ding, *J. Mol. Catal.* **2023**, *539*, 113015.

[48] a) T. Mitsudome, K. Kaneda, *Green Chem.* **2013**, *15*, 2636–2654; b) C. Vriamont, T. Haynes, E. McCague-Murphy, F. Pennetreau, O. Riant, S. Hermans, *J. Catal.* **2015**, *329*, 389–400.

[49] J. Hajek, N. Kumar, P. Maki-Arvela, T. Salmi, D. Y. Murzin, *J. Mol. Catal. A* **2004**, *217*, 145–154.

[50] a) A. B. Dongil, B. Bachiller-Baeza, A. Guerrero-Ruiz, I. Rodríguez-Ramos, *J. Catal.* **2011**, *282*, 299–309; b) C. Vriamont, T. Haynes, E. McCague-Murphy, F. Pennetreau, O. Riant, S. Hermans, *J. Catal.* **2015**, *329*, 389–400.

[51] X. Chen, H. Zhu, X. Song, H. Du, T. Wang, Z. Zhao, Y. Ding, *React. Kinet. Mech. Catal.* **2017**, *120*, 637–649.

[52] a) E. Langkopf, D. Schinzer, *Chem. Rev.* **1995**, *95*, 1375–1408; b) K. Matsumoto, J. Huang, Y. Naganawa, H. Guo, T. Beppu, K. Sato, S. Shimada, Y. Nakajima, *Org. Lett.* **2018**, *20*, 2481–2484.

[53] H. Kinoshita, R. Uemura, D. Fukuda, K. Miura, *Org. Lett.* **2013**, *15*, 5538–5541.

[54] A. Mori, E. Takahisa, Y. Yamamura, T. Kato, A. P. Mudalige, H. Kajiro, K. Hirabayashi, Y. Nishihara, T. Hiyama, *Organometallics* **2004**, *23*, 1755–1765.

[55] H. Sasabe, N. Kihara, K. Mizuno, A. Ogawa, T. Takata, *Tetrahedron Lett.* **2005**, *46*, 3851–3853.

[56] J. Zhang, G. Lu, C. Cai, *Green Chem.* **2017**, *19*, 2535–2540.

[57] a) Z. Mo, J. Xiao, Y. Gao, L. Deng, *J. Am. Chem. Soc.* **2014**, *136*, 17414–17417; b) C. Wu, W. J. Teo, S. Ge, *ACS Catal.* **2018**, *8*, 5896–5900; c) Z. Zuo, J. Yang, Z. Huang, *Angew. Chem. Int. Ed.* **2016**, *55*, 10839–10843.

[58] Y. B. Zhou, Z. K. Liu, X. Y. Fan, R. H. Li, G. L. Zhang, L. Chen, Y. M. Pan, H. T. Tang, J. H. Zeng, Z. P. Zhan, *Org. Lett.* **2018**, *20*, 7748–7752.

[59] R. H. Li, X. M. An, Y. Yang, D. C. Li, Z. L. Hu, Z. P. Zhan, *Org. Lett.* **2018**, *20*, 5023–5026.

[60] a) I. M. Abrams, *US Patent 3122514* **1964**; b) H. Corte, E. Meier, *US Patent 3586646* **1971**.

[61] a) E. B. Anderson, M. R. Buchmeiser, *ChemCatChem* **2012**, *4*, 30–44; b) J. Zhang, J. Chen, S. Peng, S. Peng, Z. Zhang, Y. Tong, P. W. Miller, X. P. Yan, *Chem. Soc. Rev.* **2019**, *48*, 2566–2595.

[62] I. M. Abrams, J. R. Millar, *React. Funct. Polym.* **1997**, *35*, 7–22.

[63] Z. Xu, Q. Zhang, H. H. Fang, *Crit. Rev. Env. Sci. Tec.* **2003**, *33*, 363–389.

[64] a) E. C. Peters, F. Svec, J. M. J. Fréchet, *Adv. Mater.* **1999**, *11*, 1169–1181; b) F. Svec, *J. Sep. Sci.* **2004**, *27*, 747–766.

[65] a) E. G. Vlakh, V. A. Korzhikov, T. B. Tennikova, *Russ. Chem. Bull.* **2012**, *61*, 937–961; b) R. I. Boysen, *J. Sep. Sci.* **2019**, *42*, 51–71.

[66] a) J. W. Labadie, *Curr. Opin. Chem. Biol.* **1998**, *2*, 346–352; b) N. A. Boyle, K. D. Janda, *Curr. Opin. Chem. Biol.* **2002**, *6*, 339–346.

[67] R. L. Albright, *React. Polym. Ion Exch. Sorb.* **1986**, *4*, 155–174.

[68] M. T. Gokmen, F. E. Du Prez, *Prog. Polym. Sci.* **2012**, *37*, 365–405.

[69] V. Smigol, F. Svec, J. M. J. Frechet, *Macromolecules* **1993**, *26*, 5615–5620.

[70] a) N. A. De Munck, M. W. Verbruggen, J. J. F. Scholten, *J. Mol. Catal.* **1981**, *10*, 313–330; b) N. A. De Munck, M. W. Verbruggen, J. E. De Leur, J. J. F. Scholten, *J. Mol. Catal.* **1981**, *11*, 331–342.

[71] L. A. Gerritsen, A. van Meerkerk, M. H. Vreugdenhil, J. J. F. Scholten, *J. Mol. Catal.* **1980**, *9*, 139–155.

[72] J. C. Carlu, C. Caze, *React. Polym.* **1990**, *13*, 153–160.

[73] C. U. Pittman Jr, L. R. Smith, *J. Am. Chem. Soc.* **1975**, *97*, 341–344.

[74] C. Andersson, Antonios Nikitidis, *Appl. Catal. A Gen.* **1993**, *96*, 345–354.

[75] a) T. Hjertberg, T. Hargitai, P. Reinholdsson, *Macromolecules* **1990**, *23*, 3080–3087; b) T. Hargitai, R. Isaksson, P. Reinholdsson, B. Tornell, *J. Chromatogr.* **1991**, *540*, 145–155.

[76] A. Nir, L. M. Pismen, *Chem. Eng. Sci.* **1977**, *32*, 35–41.

[77] N. B. Afeyan, N. F. Gordon, I. Mazsaroff, L. Varady, S. P. Fulton, Y. B. Yang, F. E. Regnier, *J. Chromatogr. A* **1990**, *519*, 1–29.

[78] J. A. Dodds, *J. Colloid Interface Sci.* **1980**, *77*, 317–327.

[79] J. V. Alemán, A. V. Chadwick, J. He, M. Hess, K. Horie, R. G. Jones, P. Kratochvíl, I. Meisel, I. Mita, G. Moad, S. Penczek, R. F. T. Stepto, *Pure Appl. Chem.* **2007**, *79*, 1801–1829.

[80] F. Svec, J. M. J. Fréchet, *Anal. Chem.* **1992**, *64*, 820–822.

[81] F. Svec, J. M. J. Fréche, *Ind. Eng. Chem. Res.* **1999**, *38*, 34–48.

[82] F. Svec, J. M. J. Fréchet, *Chem. Mater.* **1995**, *7*, 707–715.

[83] D. Barby, Z. Haq, *Eur. Patent 60138* **1982**.

[84] a) P. W. Small, D. C. Sherrington, *Chem. Commun.* **1989**, *21*, 1589–1591; b) P. Hainey, I. M. Huxham, B. Rowatt, D. C. Sherrington, L. Tetley, *Macromolecules* **1991**, *24*, 117–121; c) N. R. Cameron, D. C. Sherrington, L. Albiston, D. P. Gregory, *Colloid Polym. Sci.* **1996**, *274*, 592–595; d) N. R. Cameron, D. C. Sherrington, *J. Chem. Soc. Faraday Trans.* **1996**, *92*, 1543–1547; e) N. R. Cameron, D. C. Sherrington, *J. Mater. Chem.* **1997**, *7*, 2209–2212; f) M. Ottens, G. Leene, A. A. C. M. Beenackers, N. Cameron, D. C. Sherrington, *Ind. Eng. Chem. Res.* **2000**, *39*, 259–266.

[85] M. V. Rojo, L. Guetzoyan, I. R. Baxendale, *Org. Biomol. Chem.* **2015**, *13*, 1768–1777.

[86] a) K. F. Bolton, A. J. Canty, J. A. Deverell, R. M. Guijt, E. F. Hilder, T. Rodemann, J. A. Smith, *Tetrahedron Lett.* **2006**, *47*, 9321–9324; b) N. Karbass, V. Sans, E. Garcia-Verdugo, M. I. Burguete, S. V. Luis, *Chem. Commun.* **2006**, *29*, 3095–3097; c) A. Gömann, J. A. Deverell, K. F. Munting, R. C. Jones, T. Rodemann, A. J. Canty, J. A. Smith, R. M. Guijt, *Tetrahedron* **2009**, *65*, 1450–1454; d) V. Sans, F. Gelat, N. Karbass, M. I. Burguete, E. García-Verdugo, S. V. Luis, *Adv. Synth. Catal.* **2010**, *352*, 3013–3021; e) V. Sans, N. Karbass, M. I. Burguete, E. García-Verdugo, S. V. Luis, *RSC Adv.* **2012**, *2*, 8721–8728; f) R. P. Jumde, M. Marelli, N. Scotti, A. Mandoli, R. Psaro, C. Evangelisti, *J. Mol. Catal. A* **2016**, *414*, 55–61.

[87] M. I. Burguete, A. Cornejo, E. García-Verdugo, M. J. Gil, S. V. Luis, J. A. Mayoral, V. Martínez-Merino, M. Sokolova, *J. Org. Chem.* **2007**, *72*, 4344–4350.

[88] M. R. Buchmeiser, *Chem. Rev.* **2009**, *109*, 303–321.

[89] R. H. Grubbs, S. Chang, *Tetrahedron* **1998**, *54*, 4413–4450.

[90] F. Sinner, M. R. Buchmeiser, *Angew. Chem. Int. Ed.* **2000**, *39*, 1433–1436.

[91] a) M. Mayr, B. Mayr, M. R. Buchmeiser, *Angew. Chem. Int. Ed.* **2001**, *40*, 3839–3842; b) J. O. Krause, S. Lubbad, O. Nuyken, M. R. Buchmeiser, *Adv. Synth. Catal.* **2003**, *345*, 996–1004; c) M. Mayr, D. Wang, R. Kröll, N. Schuler, S. Prühs, A. Fürstner, M. R. Buchmeiser, *Adv. Synth. Catal.* **2005**, *347*, 484–492.

[92] a) C. C. C. J. Seechurn, M. O. Kitching, T. J. Colacot, V. Snieckus, *Angew. Chem. Int. Ed.* **2012**, *51*, 5062–5085; b) K. M. Korch, D. A. Watson, *Chem. Rev.* **2019**, *119*, 8192–8228; c) J. B. Diccianni, T. Diao, *Trends Chem.* **2019**, *1*, 830–844.

[93] R. L. Hartman, J. R. Naber, N. Zaborenko, S. L. Buchwald, K. F. Jensen, *Org. Process Res. Dev.* **2010**, *14*, 1347–1357.

[94] J. R. Naber, S. L. Buchwald, *Angew. Chem. Int. Ed.* **2010**, *49*, 9469–9474.

[95] H. Matsumoto, Y. Hoshino, T. Iwai, M. Sawamura, Y. Miura, *Ind. Eng. Chem. Res.* **2020**, *59*, 15179–15187.

[96] H. Matsumoto, Y. Hoshino, T. Iwai, M. Sawamura, Y. Miura, *Chem. Eur. J.* **2023**, *29*, e202301847.

[97] V. Udumula, J. H. Tyler, D. A. Davis, H. Wang, M. R. Linford, P. S. Minson, D. J. Michaelis, *ACS Catal.* **2015**, *5*, 3457–3462.
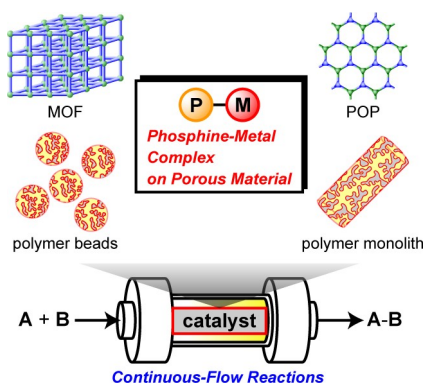
REVIEW

This review highlights the efficacy of continuous-flow syntheses using immobilized catalysts, particularly focusing on porous polymers. These polymers feature their large surface area, stability, and cost-effectiveness, making them valuable in organic chemistry. Emphasizing the immobilization of transition-metal catalysts using supported phosphine ligands, the review summarizes strategies for achieving high activities, durabilities, and selectivities in continuous-flow systems, categorizing polymer catalysts by pore size.

MOF

POP

P — M

Phosphine-Metal Complex on Porous Material

polymer beads

polymer monolith

A + B → catalyst → A-B

Continuous-Flow Reactions

Dr. H. Matsumoto, Dr. T. Iwai, Prof. Dr. M. Sawamura, Prof. Dr. Y. Miura**

1 – 14

Continuous-Flow Catalysis Using Phosphine-Metal Complexes on Porous Polymers: Designing Ligands, Pores, and Reactors